ELSEVIER

Polymer 44 (2003) 1229–1235

polymer

www.elsevier.com/locate/polymer

Transcrystallinity in brominated UHMWPE fiber reinforced HDPE composites: morphology and dielectric properties

Linda Vaisman, M. Fernanda González*, Gad Marom*

Casali Institute of Applied Chemistry, The Hebrew University of Jerusalem, Givat Ram Campus, 91904 Jerusalem, Israel

Abstract

Ultra-high-molecular-weight polyethylene (UHMWPE) fibers were treated by photochemical bromination. The analysis of the fibers by XPS and ATR-FTIR showed that this process led to the introduction of C–Br and C–OH moieties and generated C=C bonds at the PE fiber surface.

Composites were fabricated using either treated or untreated fibers and high-density polyethylene (HDPE) for the matrix. WAXD analysis showed that the treated fibers, through offering a higher concentration of crystallization nuclei, generated a denser transcrystalline layer with higher specific radial orientation with respect to the fiber axis—compared with the untreated fiber. Furthermore, the introduction of polarity onto the fiber surface enabled analysis of the complex relaxation behavior of PE/PE composites by dielectric spectroscopy. It showed the typical α, β and γ-relaxation processes of polyethylene, combined with the effect of the transcrystalline layer, generating—among other changes—a strong β-transition.

Keywords: UHMWPE composites; Transcrystallinity; Dielectric spectroscopy

1. Introduction

Since their invention in 1975 [1], the so-called self-reinforced, single-polymer composites—based on Ultra-high-molecular-weight polyethylene (UHMWPE) fibers in a PE matrix—have been studied extensively with different types of PE matrices and a range of length and orientation of the fibers [2–5]. The identical chemical nature and crystalline morphology of the constituents in this composite system result in their mutual compatibility at the interface. This generates, in addition to a relatively good interfacial adhesion, a unique fiber/matrix interface, wherein the matrix crystallizes preferentially on the fiber surface to produce a transcrystalline cylindrical interfacial layer [6–9]. Recent studies have shown that a dense transcrystalline layer nucleates epitaxially on the fiber surface and grows radially relative to the fiber axis in a mechanism that involves lamella twisting [10,11].

A variety of experimental techniques has been utilized, including X-ray diffraction, electron and light microscopy and dynamic mechanical analysis, to study transcrystallization in a wide range of composite materials. In addition, dielectric spectroscopy has been employed successfully to analyze the nature of phase transitions in transcrystallinity in aramid fiber reinforced nylon 66 [12] and PEEK composites [13]. The latter technique is not very useful for PE–PE composites, which are practically inert in an electric field, having a significant lower dielectric constant compared with polar polymers. So, it is the same property that makes PE–PE composites attractive candidates for various electronic applications that inhibits the utilization of dielectric spectroscopy analysis to study phase transitions.

The present study has been driven by the idea that a specifically selected surface treatment of the PE fiber can generate a double effect, wherein the polarity of the fiber surface is increased and the transcrystalline morphology is modified. It has been hypothesized that surface bromination of the PE fiber can implant polar moieties on the fiber surface which will serve to both enhance matrix nucleation and transcrystallization and increase the dielectric activity of the system. Thus, the aim of this work is to use dielectric spectroscopy to study phase transitions in transcrystallinity of PE–PE composites, to be done by increasing the polarity of the fiber surface via bromination and by subsequently growing a transcrystalline layer of enhanced dielectric response.

* Tel.: +972-2-658-5898; fax: +972-2-658-6068 (G. Marom).
* Tel.: +972-2-658-6572 (M. Fernanda González).
E-mail addresses: fernanda@vms.huji.ac.il (M. Fernanda González), gadm@vms.huji.ac.il (G. Marom).

0032-3861/03/$ - see front matter © 2002 Elsevier Science Ltd. All rights reserved.
PII: S0032-3861(02)00848-0

2. Materials and methods

2.1. Fiber surface treatment

Spectra-1000 (Allied Signal) UHMWPE fibers were used. Bromine was purchased from Merck and was used without further purification.

PE fibers were suspended inside a Quartz tube previously purged with dry nitrogen gas during 10 min and immediately closed. Two drops of bromine were injected into the tube through a rubber septum and allowed to evaporate. The fibers were exposure to the bromine atmosphere for predetermined periods of time. Next, the tube was placed at a distance of 5–10 cm from an UV-C lamp (Vilber Lournat 6 W; 254 nm,) and irradiated for 30 s. After the irradiation the fibers were put in a vacuum oven overnight to eliminate the non-reacted bromine. The fibers were kept in a nitrogen-purged vessel until use.

2.2. Microcomposite preparation

For the matrix, films were prepared by pressing Du Pont Sclair 2909 high-density polyethylene (HDPE), using a Carver hydraulic press, model 2518, at 150 °C with a pressure of 1.5 MPa. Films of approximately 80 μm thickness were obtained.

Microcomposites were fabricated by aligning approximately 30 UHMWPE monofilaments on a HDPE film using a special device described elsewhere [14], which were, in turn, placed either between two glass slides and inserted in a hot stage (Mettler FP82), or between two Kapton films and pressed in a laboratory press. This second method was used in order to process larger pieces and to prevent air-bubbles formation in the samples that were prepared for testing the dielectric properties. The fibers were fixed by their extremes in order to minimize the relaxation process and thus, prevent fiber melting. The composite was heated and held at 137 °C for 30 min followed by cooling at a rate of 2 °C/min to 127 °C for isothermal treatment and subsequently quenching in ice-water.

2.3. Characterization

Attenuated total reflectance-FTIR (ATR-FTIR) spectra were collected on a Nicolet 510 FTIR spectrometer equipped with a ZnSe crystal at 45°.

X-ray photoelectron spectroscopy (XPS) analyses were performed using a UHV (2.5×10^{-10} torr base pressure) with 5600 Multi-Technique System from PHI, USA, equipped with a spherical capacitor analyzer with slit aperture of 800 μm. Al Kα radiation (monochromator source 1486.6 eV) was used.

Visual examination of the composites was achieved, either by using a Nikon optical microscope equipped with cross polarizers and by performing electron microscopy in a JEOL JSM 840 scanning electron microscope (SEM) after permanganic etching of the samples, according to a previously reported process [15].

Wide angle X-ray diffraction (WAXD) patterns were obtained on Fuji imaging plates, using a Searle camera equipped with Franks optics affixed to an Elliot GX6 rotating Cu anode generator operating at 1.2 kW. The X-ray beam was nickel filtered ($\lambda = 1.54$ Å) and was about 400 μm in diameter in the plane of the sample. The exposure time was 3 h.

Dielectric measurements were carried out by using a broad band electric spectrometer BDS 4284 (Novocontrol) with automatic temperature control in the range of −150–100 °C. The samples were coated with silver paint to improve the contact with the electrodes.

3. Results and discussion

3.1. Fiber surface modification

The creation of dipoles at the surface of the UHMWPE fiber was attempted in this study through a photobromination process previously reported in the literature for LDPE [16]. The technique, based on simultaneous exposure of the PE substrate to bromine atmosphere and UV-C radiation, was expected to generate C–Br dipoles on the PE fiber surface. Both ATR-FTIR and XPS analyses were employed to analyze the as received fibers before and after the bromination process.

Fig. 1 shows the ATR-FTIR spectra of treated and untreated fibers. It is possible to observe the appearance of two distinct peaks in the spectra of the fibers after bromination at 3300 and at 1645 cm^{-1}, corresponding to C–OH and C=C bonds, respectively. It is also noted that the peaks present in the untreated PE fibers, which correspond to the CH_2 and CH_3 different absorbance, diminish after treatment. Unfortunately, equipment limitations prevented

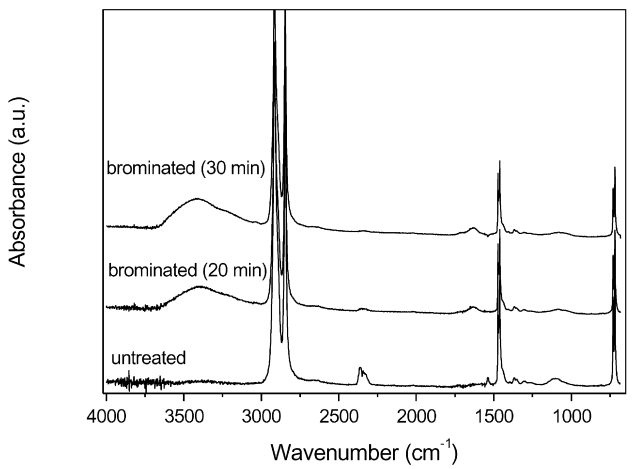

Fig. 1. ATR-FTIR of the fibers before and after 20 and 30 min of exposure to bromine gas and irradiated for 30 s with UV-C light.

detailed analysis of the 550, 568 and 620 cm^{-1} absorbance of the C–Br bond [17].

Table 1 displays the fiber surface atomic composition obtained by XPS for several treatments. It is seen that approximately 1.4 at.% of bromine was introduced to the fiber surface, regardless of the exposure time to bromine. A similar behavior—yet with a larger yield of substitution—was previously reported for the bromination of LDPE [18]. That study of the bromination of LDPE [16,18] showed that increased bromination time resulted in more extensive surface damage with no effect on the amount of bromine grafted to the LDPE.

In agreement with the FTIR results, the oxygen concentration on the fiber surface increased after bromination independently of the exposure duration. The oxygen concentration did not change even in samples, which after exposure to bromine were irradiated in the presence of atmospheric oxygen. It is, therefore, plausible that the oxygen source is not atmospheric: it is either molecular oxygen or water present in the fiber. Other studies showed that significant concentrations of oxygen existed even after treating the fiber under inert atmosphere [16] and that irradiating with a short wave UV light promoted oxidation [19].

An analysis of the XPS results for the O1s level shown in Fig. 2 indicates that the surface oxygen in the untreated fibers is ascribed to C–OH and C=O groups, observed at 533 and 530 eV, respectively. After exposing the fiber to bromine and UV radiation the atomic percentage of oxygen at the fiber surface increases 5-fold to ~9%, present mainly in the form of C–OH group.

At least two mechanisms can explain the oxidation of the PE fiber under the combined action of bromine and UV radiation that generates photolysis of the Br_2 molecule to produce Br radicals. While the main bromination reaction proceeds through abstraction of hydrogen radical off the polyethylene chain and the eventual formation of C–Br groups, chain radicals and Br radicals can react with molecular oxygen and water, respectively. Molecular oxygen is known to be an inhibitor for free radical reactions by reacting with the radicals that are formed during bromination, creating peroxide radicals that compete for the hydrogen abstraction [20]. The presence of oxygen leads to chain scission, crosslinking and formation of various oxygen-containing species [21]. In a similar way the oxygen can

Table 1
Atomic composition of the fiber surface before and after photochemical bromination, measured by XPS (at %)

UHMWPE fibers	C	O	Br
Untreated	98.2	1.8	–
20 min in bromine gas; 30 s UVC irradiation	89.4	9.2	1.4
60 min in bromine gas; 30 s UVC irradiation	89.1	9.6	1.3
No exposure to bromine gas; 30 s UVC irradiation	90.8	9.2	0.0
20 min in bromine gas; 30 s UVC irradiation in air	89.9	9.2	0.9

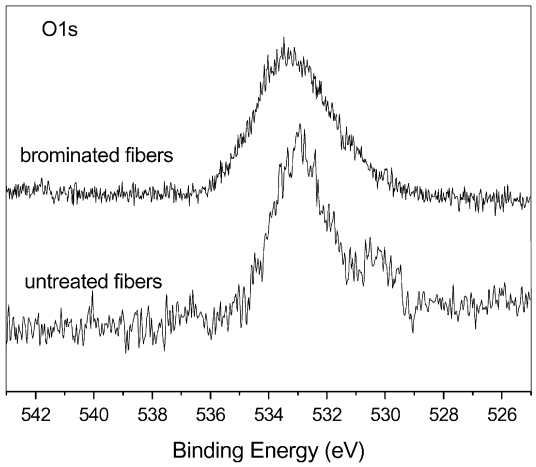

Fig. 2. XPS spectra of untreated and photochemical brominated fibers, the O1s level.

catalyze the dehydrobromination during the bromination process, creating C=C bonds [17]. Furthermore, Br radicals can react with water molecules to form hydroxyl radicals that can then attack the polyethylene chain or couple with a previously formed chain radical [18].

Regardless of the mechanism of surface oxidation of the PE fiber, the addition of C–OH beside the C–Br groups to the fiber surface, served the purpose of raising the surface polarity and of increasing the dielectric activity, to enable the anticipated study of PE transcrystallinity by dielectric spectroscopy.

3.2. The transcrystalline layer

Fig. 3a and b shows SEM pictures of the interfacial region of composites prepared using untreated and 20 min brominated fibers, respectively. Both samples were identically etched with permanganic solution. Both fibers generated a thick transcrystalline layer (of the order of the fiber width), which had apparently nucleated integrally with the fiber skin and grew to form a continuum of fiber and transcrystallinity. It is possible to observe the radially oriented lamellae relative to the fiber axis with some apparent evidence of lamella twisting. It can be observed that the transcrystalline layer around the brominated sample is slightly denser and more compact. It is interesting to note that the UHMWPE fiber has a bean-shaped (and not circular) cross-section. And, whereas the fiber in Fig. 3a exhibits its convex side, the treated one in Fig. 3b exhibits its concave side, showing an ordered transcrystalline layer within the concave cavity.

Our group has studied extensively the transcrystalline layer of HDPE around UHMWPE fibers, its morphology and its influence on the mechanical properties of the composites [8,10,22,23]. Transcrystallinity of HDPE had the same crystalline morphology of the bulk spherulites, depending on the thermal history. Epitaxial nucleation at the fiber surface occurred so that the lamella *c*-axis (the chain

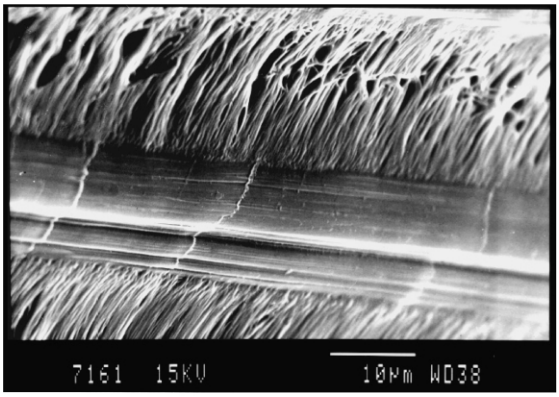

a

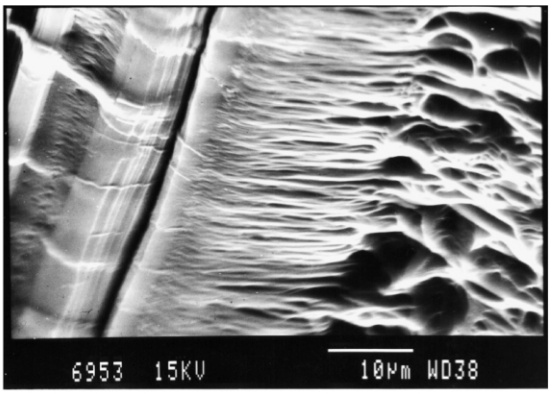

b

Fig. 3. SEM pictures of the transcrystalline interfacial region in composites based on (a) untreated fibers, and (b) surface modified fibers.

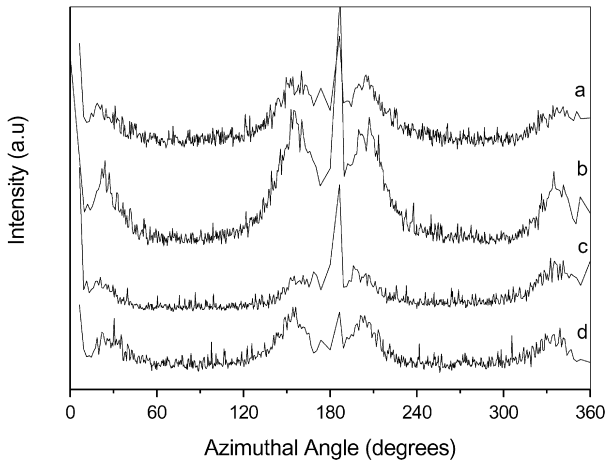

Fig. 4. Histograms of the Azimuthal angle distribution of the (110) reflection obtained from the WAXD patterns of microcomposites with (a) untreated fibers and 12 μm transcrystallinity; (b) 20 min brominated fibers and 12 μm transcrystallinity; (c) untreated fibers and 7.5 μm transcrystallinity; (d) 20 min brominated fibers and 7.5 μm transcrystallinity.

axis) was parallel to the fiber axis. In all the cases the transcrystalline layer exhibited an oriented crystalline structure in which the orthorhombic crystalline lamellae grew radially into the matrix bulk. The growth proceeded by lamella twisting, wherein the $a-c$ plane rotated around the b-axis (growth direction). The pitch of the lamellar twist was calculated to be 28.6 μm [10].

In order to quantify the crystalline order within the transcrystalline layer, WAXD was performed with unidirectional microcomposites comprising transcrystalline layers of either 7.5 or 12.0 μm thick, obtained during isothermal crystallization times of 20 and 60 min, respectively. The 2D diffraction patterns were exactly similar to those shown by Stern et al. [8], and like previously, the (110) and (200) highest intensity orthorhombic diffraction rings were analyzed by generating histograms of the angular intensity distribution around the rings. Fig. 4 presents such histograms of the (110) reflection of four samples of treated and untreated fibers and two transcrystalline layer thicknesses (note that the 0 and 180° angles mark the equatorial, while the 90 and 270° mark the meridian position). Each peak was then fitted with the best Gaussian distribution and its full-width at half-maximum (FWHM) was calculated. Obviously, narrower peaks, corresponding to shorter arcs in the diffraction image, reflect a higher crystalline order and more distinctive lamella orientation. The results of the analysis are presented in Table 2 for the two diffraction rings. It is seen that peaks of the transcrystalline layers of the brominated fibers are always narrower. For example, in the brominated fiber composites with 12.0 μm transcrystallinity the diffraction arc was 22 ± 4 and 17 ± 9% narrower for the (110) and (200) reflection, respectively. Thus, the WAXD results provide strong support to the SEM observations above, that the surface treated fibers induce a denser more oriented transcrystalline interfacial layer.

3.3. Dielectric properties

The relaxation processes and phase transitions of PE have been studied extensively, mostly by dynamic mechanical analysis, identifying classically three main transitions, named conventionally α, β and γ, from higher to lower temperature.

The α-transition is related to the chain movements within the crystal phase, but the molecular mechanisms involved in this process are still not clear. This transition occurs usually in the temperature range of 30–120 °C, and its specific location (as well as the appearance of a related α′-transition) is determined by the lamellar thickness [24–26]. The origin of β-transition is still a controversial issue. This transition is found in the region of −30–10 °C and is attributed to the motion of loose folds and relatively non-extended tie chains present in the lamellar interface, and it is, therefore, more pronounced in LDPE or in modified HDPE [24,26]. Some authors attribute the β-relaxation to the glass transition [25,27]. The γ-relaxation is usually associated with the glass transition [24,28], yet few authors assign it specifically to the crankshaft movements of three methylene unit segments in the amorphous region [27,29,30].

Fig. 5a and b presents a comparative overview of the

Table 2
Full-width at half-maximum of each maximum in the histograms of the angular intensity distribution (calculated from the WAXD data) fitted with the best Gaussian distribution for the (110) and (200) reflections

Plane	Composite type transcrystalline thickness	FWHM (degree)			
		Peak #1	Peak #2	Peak #3	Peak #4
(110)	PE–PE; 12 μm	20.6	20.7	20.1	21.1
	Br/PE–PE; 12 μm	15.6	16.9	15.7	15.9
	PE–PE; 7.5 μm	28.4	26.3	26.1	27.2
	Br/PE–PE; 7.5 μm	20.5	23.8	24.0	20.9
(200)	PE–PE; 12 μm	34.0	41.2	41.7	34.0
	Br/PE–PE; 12 μm	28.7	30.9	31.9	32.0
	PE–PE; 7.5 μm	57.9	39.1	40.2	57.7
	Br/PE–PE; 7.5 μm	56.1	36.2	38.3	55.1

The peaks are numbered 1–4 from low to high angle.

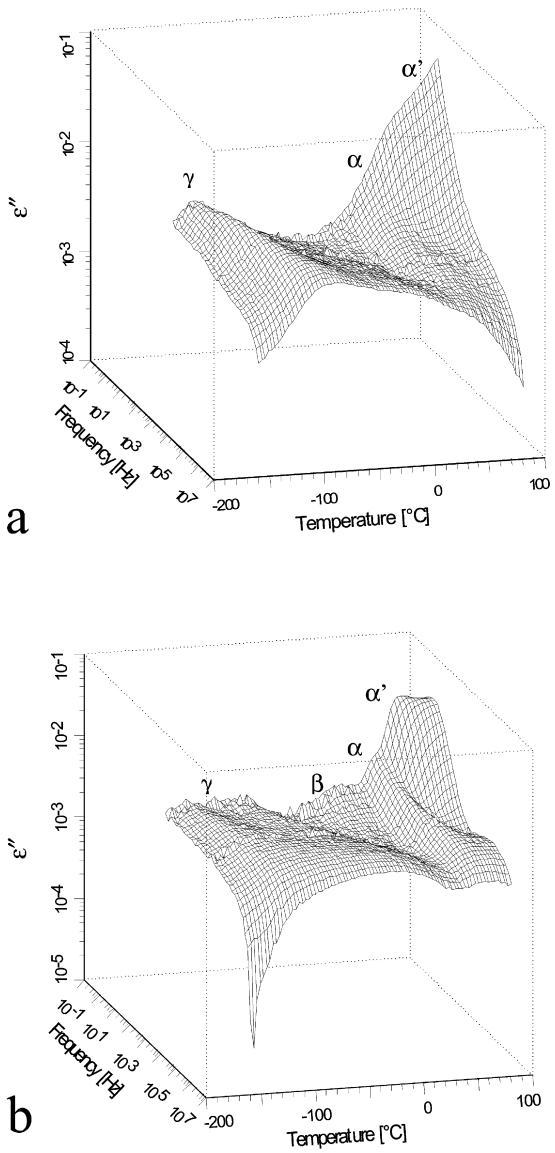

Fig. 5. Dielectric loss (ε'') of microcomposites based on (a) untreated fibers; (b) 20 min brominated fibers.

dielectric loss (ε'') as a function of temperature and frequency for composites with untreated fibers and brominated/oxidized fibers, respectively. The main observable differences between the untreated and treated composite is that the latter exhibits a more pronounced α-relaxation, a fairly significant β-relaxation over a wide frequency range, and a γ-relaxation that is less sharp and spread over a wider temperature range. The differences between the untreated and treated fiber composites become clearer when the results are examined at four particular frequencies as shown in Fig. 6. Based on our previous study—by dynamic mechanical analysis—of the effect of transcrystallinity on the relaxation processes in PE fiber-reinforced PE [28], we can now see how explicit features of the dielectric spectrum which are typical of transcrystallinity are intensified by the fiber treatment. And, the effect of the ordered transcrystallinity on the relaxation processes can be explained by considering the specific molecular motion associated with each relaxation process. A more pronounced α-relaxation (and α'-relaxation at the lower frequency range), observed for the treated fiber composites, is indicative of thicker lamellae. A significant β-relaxation over a wide frequency range is associated with motion of loose folds at the lamella surface. This relaxation is not visible in HDPE, due to its tight folded chain structure, and also not in the extended chain UHMWPE fiber. A less sharp, less explicit γ-relaxation (glass transition) peak that is shifted to a higher temperature (around $-50\,^{\circ}C$) over a wide frequency range reflects a more restricted main chain segmental mobility which is imposed by transcrystallinity.

Fig. 7 shows the dielectric loss (ε'') as a function of frequency at three different temperatures for composites with untreated and brominated/oxidized fibers. At $-100\,^{\circ}C$ the γ-relaxation (glass transition) is seen to be largely frequency independent (Fig. 7a), exhibiting lower intensity in the treated fiber composite. The frequency–temperature dependence for the glass transition process is usually described in terms of an Arrhenius-type equation. The calculated activation energies for the γ-relaxation were

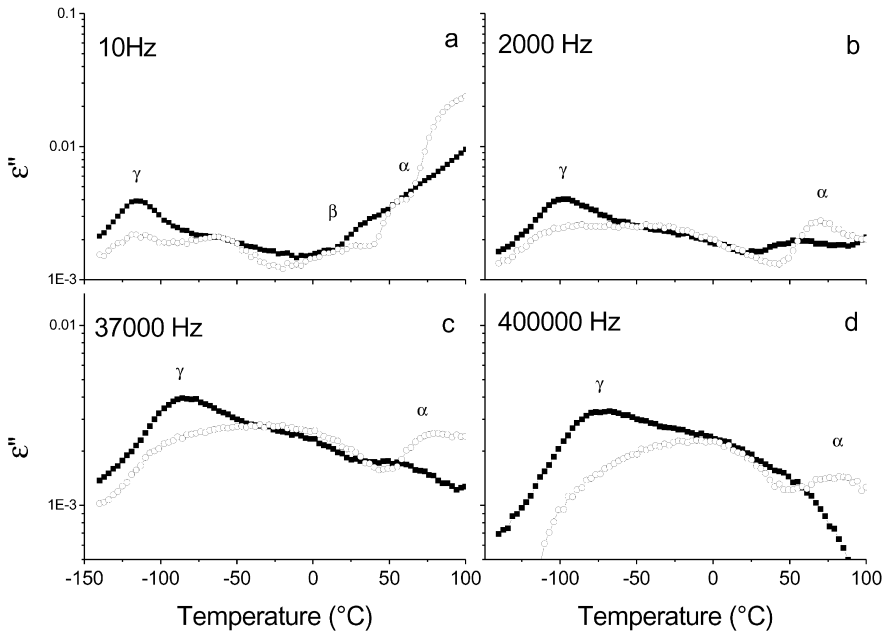

Fig. 6. Dielectric loss (ε'') as a function of the temperature at (a) 10 Hz; (b) 2000 Hz; (c) 37,000 Hz and (d) 400,000 Hz. (-■-) Composite with untreated fibers; (-○-) composite with brominated fibers.

30.5 kJ/mol and 44.9 kJ/mol in the untreated fiber and brominated/oxidized fiber composites, respectively. The higher activation energy indicates that the molecular motion in the amorphous phase of the treated fiber composite is more restricted, apparently as a consequence of the denser and more organized transcrystallinity. This is in agreement with the previously observed effect of transcrystallinity versus that of bulk crystallinity on the activation energy [12, 28]. The dielectric relaxation behavior at 20 °C (Fig. 7b) show a clear β-relaxation for the treated fiber composite in the low frequency range, whereas the untreated fiber composite does not exhibit any relaxation at this temperature. Finally, at 80 °C (Fig. 7c) the α-relaxation appears, presented in both composites at low and high frequencies. It can be seen clearly that the treated fiber composite presents a higher intensity transition. The activation energies of the α-relaxation (calculated as explained above for the γ-relaxation) were 161 and 141 kJ/mol in the untreated fiber and brominated/oxidized fiber composites, respectively. As the α-relaxation is conventionally assigned to segmental chain motion in the lamella, it can be suggested that this motion is less restricted in the thicker transcrystalline lamella of the treated fiber composite. Correspondingly, it was found previously that the induction of orientation decreased the activation energy of the α-transition in the dynamic-mechanical response of HDPE [31].

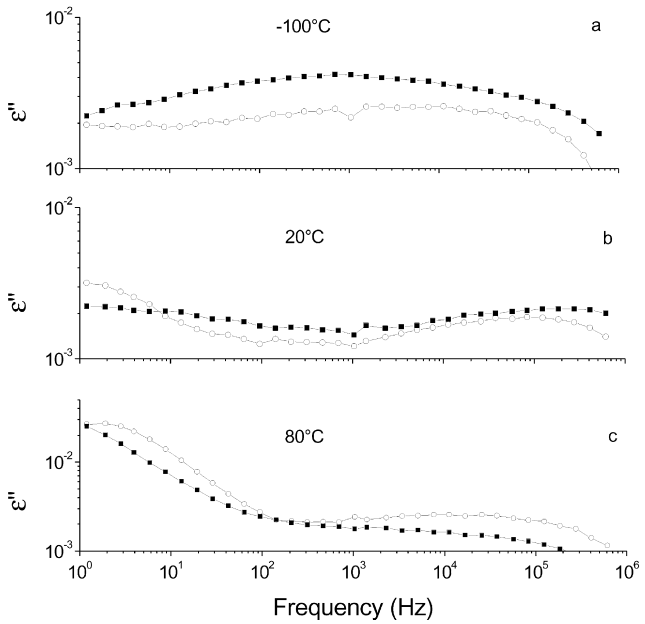

Fig. 7. Dielectric loss (ε'') as a function of the frequency at (a) − 100 °C; (b) 20 °C; and (c) 80 °C. (-■-) Composite with untreated fibers; (-○-) composite with brominated fibers.

4. Conclusions

The photochemical bromination of UHMWPE fibers, which produces C−Br groups on the fiber surface, is accompanied by the formation of C−OH and C=C groups. Quantitatively, the surface treatment results in concentrations of 1.4 and 9.2 at.% of bromine and oxygen, respectively.

The bromination/oxidation process increases the nucleation density of the HDPE matrix on the fiber surface, thus generating a denser more ordered transcrystalline layer compared with the untreated fiber composite.

The typical relaxation characteristics of transcrystallinity in PE−PE composites—such as a more pronounced α-relaxation, a significant β-relaxation over a wide frequency

range, and a subdued γ-relaxation—are intensified in the treated fiber composites, confirming the ability of the treated fiber to produced exceedingly ordered transcrystallinity.

Acknowledgements

The authors gratefully acknowledge Prof. Yuri Feldman and his group for the help on the dielectric spectroscopy experiments.

References

[1] Capiati NJ, Porter RS. J Mater Sci 1975;10:1671–7.
[2] Stern T, Teishev A, Marom G. Compos Sci Technol 1997;57:1009–15.
[3] Kazanci M, Cohn D, Marom G. J Mater Sci 2001;36:2845–50.
[4] Devaux E, Cazé C. Compos Sci Technol 1999;59:459–66.
[5] Marais G, Feillard P. Compos Sci Technol 1992;45:247–55.
[6] He T, Porter RS. J Appl Polym Sci 1988;35:1945–53.
[7] Ishida H, Bussi P. Macromolecules 1991;24:3569–77.
[8] Stern T, Marom G, Watchel E. Composites, Part A 1997;28A:437–44.
[9] Lacroix FV, Loos J, Schulte K. Polymer 1999;40:843–7.
[10] Stern T, Watchel E, Marom G. J Polym Sci, Part B: Polym Phys 1997;35:2429–33.
[11] Flores A, Poeppel A, Riekel C, Schulte K. J Macromol Sci, Phys 2001;B40:749–61.
[12] Nuriel H, Kozlovich N, Feldman Y, Marom G. Composites, Part A 2000;31:69–78.
[13] Korbakov N, Harel H, Feldman Y, Marom G, Macromol Chem Phys; submitted for publication.
[14] Wagner HD, Steenbakkers LW. J Mater Sci 1989;24:3956–75.
[15] Basset DC, Olley RH. Polymer 1984;25:935.
[16] Chanunpanich N, Ulman A, Strzhemechny YM, Schwartz SA, Janke A, Braun HG, Kraztmuller T. Langmuir 1999;15:2089–94.
[17] Balamurugan S, Mandale AB, Badrinarayanan S, Vernekar SP. Polymer 2001;42:2501–12.
[18] Chanunpanich N, Ulman A, Malagon A, Strzhemechny YM, Schwartz SA, Janke A, Kraztmuller T, Braun HG. Langmuir 2000;16:3557–60.
[19] Peacock AJ. Handbook of polyethylene, structures, properties and applications. New York: Marcel Dekker; 2000. p. 396.
[20] March J. Advanced organic chemistry. Reactions mechanisms and structure, 4th ed. New York, USA: Wiley; 1992. Chapter 14.
[21] Sanderson RD, du Toit FJ, Carstens PAB, Wagener IB. J Therm Anal 1994;41:563–81.
[22] Teishev A, Marom G. J Appl Polym Sci 1995;56:959–66.
[23] Levitus D, Kenig S, Kazanci M, Harel H, Marom G. Adv Compos Lett 2001;10:61–5.
[24] Laredo E, Suarez N, Bello A, Rojas de Gáscue B, Gomez MA, Fatou JMG. Polymer 1999;40:6405–16.
[25] Ward IM, Hadley DW. An introduction to the mechanical properties of solid polymers. Chichester, England: Wiley; 1993. Chapter 9.
[26] Sirotkin RO, Brooks NW. Polymer 2001;42:9801–8.
[27] Boyd RH, Liu F. In: Runt JP, Fitzgerald JJ, editors. Dielectric spectroscopy of polymeric materials. Fundamentals and applications. USA: ACS publisher; 1997. Chapter 4.
[28] Pegoretti A, Ashkar M, Migliaresi C, Marom G. Compos Sci Technol 2000;60:1181–9.
[29] Suljovrujic E, Kacarevic-Popovic Z, Kostoki D, Dojcilovic J. Polym Degrad Stability 2001;71:367–73.
[30] Cerrada ML, Pereña R, Benavente R, Pérez E. Polymer 2000;41:6655–61.
[31] Mano JF, Sousa RA, Reis RL, Cunha AM, Bevis MJ. Polymer 2001;42:6187–98.